

Isotopic Composition of Atmospheric Mercury in China: New Evidence for Sources and Transformation Processes in Air and in Vegetation

Ben Yu,^{†,‡} Xuewu Fu,^{*,†} Runsheng Yin,[†] Hui Zhang,[†] Xun Wang,^{†,‡} Che-Jen Lin,^{†,§} Chuansheng Wu,^{‡,||} Yiping Zhang,^{||} Nannan He,[⊥] Pingqing Fu,[⊥] Zifa Wang,[⊥] Lihai Shang,^{*,†} Jonas Sommar,[†] Jeroen E. Sonke,[#] Laurence Maurice,[#] Benjamin Guinot,[∇] and Xinbin Feng^{*,†}

[†]State Key Laboratory of Environmental Geochemistry, Institute of Geochemistry, Chinese Academy of Sciences, Guiyang 550002, China

[‡]University of Chinese Academy of Sciences, Beijing 100049, China

[§]Department of Civil and Environmental Engineering, Lamar University, Beaumont, Texas United States

^{||}Key Laboratory of Tropical Forest Ecology, Xishuangbanna Tropical Botanical Garden, Chinese Academy of Sciences, Mengla, 666303, China

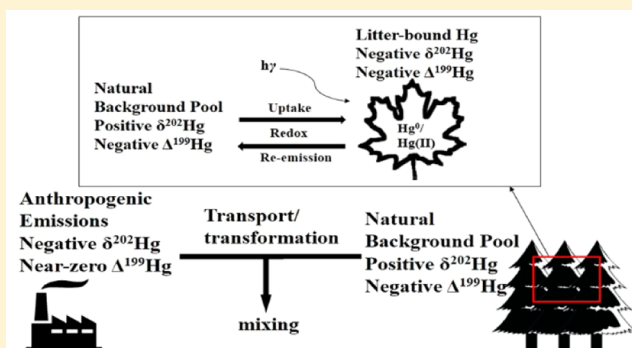
[⊥]State Key Laboratory of Atmospheric Boundary Layer Physics and Atmospheric Chemistry, Institute of Atmospheric Physics, Chinese Academy of Sciences, Beijing 100029, China

[#]Observatoire Midi-Pyrénées, Laboratoire Géosciences Environnement Toulouse, CNRS/IRD/Université Paul Sabatier, 14 Avenue Edouard-Belin, 31400 Toulouse, France

[∇]Laboratoire d'Aérodologie, Université de Toulouse, CNRS, UPS, 14 Avenue Edouard-Belin, 31400 Toulouse, France

Supporting Information

ABSTRACT: The isotopic composition of atmospheric total gaseous mercury (TGM) and particle-bound mercury (PBM) and mercury (Hg) in litterfall samples have been determined at urban/industrialized and rural sites distributed over mainland China for identifying Hg sources and transformation processes. TGM and PBM near anthropogenic emission sources display negative $\delta^{202}\text{Hg}$ and near-zero $\Delta^{199}\text{Hg}$ in contrast to relatively positive $\delta^{202}\text{Hg}$ and negative $\Delta^{199}\text{Hg}$ observed in remote regions, suggesting that different sources and atmospheric processes force the mass-dependent fractionation (MDF) and mass-independent fractionation (MIF) in the air samples. Both MDF and MIF occur during the uptake of atmospheric Hg by plants, resulting in negative $\delta^{202}\text{Hg}$ and $\Delta^{199}\text{Hg}$ observed in litter-bound Hg. The linear regression resulting from the scatter plot relating the $\delta^{202}\text{Hg}$ to $\Delta^{199}\text{Hg}$ data in the TGM samples indicates distinct anthropogenic or natural influences at the three study sites. A similar trend was also observed for Hg accumulated in broadleaved deciduous forest foliage grown in areas influenced by anthropogenic emissions. The relatively negative MIF in litter-bound Hg compared to TGM is likely a result of the photochemical reactions of Hg^{2+} in foliage. This study demonstrates the diagnostic stable Hg isotopic composition characteristics for separating atmospheric Hg of different source origins in China and provides the isotopic fractionation clues for the study of Hg bioaccumulation.



INTRODUCTION

Mercury (Hg), released to atmosphere by both anthropogenic and natural emissions, is a global pollutant posing a threat to the health of humans and wildlife.¹ Hg emissions in China account for approximately one-third of anthropogenic mercury emissions to the global atmosphere.^{2,3} Although with uncertainty,^{4,5} Hg release from natural surfaces including re-emissions of legacy Hg from terrestrial landscapes in China have been considered significantly elevated compared to that reported in Europe and North America.³ Source attribution of atmospheric Hg is

challenging due to the unique characteristics of the dominant Hg^0 species, such as its long residence time in the atmosphere (0.5–1 years), tendency to revolatilize after deposition, mixing ratios below parts per trillion (pptv),⁶ and not yet well understood bidirectional exchange between the atmosphere and terrestrial surfaces.⁴

Received: April 11, 2016

Revised: July 6, 2016

Accepted: August 2, 2016

Published: August 2, 2016

Since the development of multicollector inductively coupled plasma mass spectrometry (MC-ICPMS), the composition of stable Hg isotopes has been investigated for the source apportionment of Hg in environmental compartments. Hg isotopes exhibit both mass-dependent fractionation (MDF) and mass-independent fractionation (MIF). Hg-MDF (reported as $\delta^{202}\text{Hg}$) has been demonstrated to ubiquitously occur in the environment as a result of chemical,^{7–11} physical,^{12–17} and biological processes,^{7,18–23} while Hg-MIF is triggered only by specific mechanisms. Recent studies also reported MIF (calculated by relating with $\delta^{202}\text{Hg}$) for both odd (e.g., ^{199}Hg and ^{201}Hg) and even (e.g., ^{200}Hg , ^{204}Hg) isotopes. The odd-MIF (reported here as $\Delta^{199}\text{Hg}$) results primarily from, for example, aqueous photochemical reactions.^{7–10,21,22} Significant even-MIF (reported here as $\Delta^{200}\text{Hg}$), hypothesized to be caused by atmospheric Hg⁰ photo-oxidation, has been observed in atmospheric precipitation and surface waters.^{24–26} Hence, Hg isotope measurements may reveal diagnostic patterns of multiple useful isotopic signatures ($\delta^{202}\text{Hg}$ – $\Delta^{199}\text{Hg}$ – $\Delta^{200}\text{Hg}$ – $\Delta^{201}\text{Hg}$), and therefore provide clues for tracing sources and pathways related to Hg transport and transformation.

Source attribution of atmospheric Hg by exploring isotopic signatures in samples coupled with meteorological analysis is conceivable since the isotopic compositions of anthropogenic Hg emission sources are potentially different from each other.^{27,28} However, the isotopic composition of atmospheric Hg is not well constrained at a sufficient spatial-temporal coverage. This especially concerns particle-bound Hg (PBM) due to the challenge in sampling and preconcentration from ambient air. In addition, a large variation of speciated atmospheric Hg isotopic compositions has been reported in earlier studies, suggesting a complex interaction of sources, mixing, and transformation processes in shaping the isotopic composition of airborne Hg.^{24,27,29} Sufficient fundamental isotopic data on atmospheric Hg from sources and receptors is crucial for the application of Hg isotopes in Hg source apportionment and processes analysis.

Hg isotopic compositions in foliage and lichen/moss has been utilized as a proxy to reflect the bulk Hg isotopic compositions of ambient air.^{30,31} However, recent direct measurements of airborne Hg exhibited a substantial isotopic discrepancy between vegetation and air samples and suggested important isotopic fractionation during exchange and assimilation.^{23,26,32} Since isotopic fractionation, especially MIF of Hg, points to diagnostic geochemical processes, more detailed isotopic data may provide clues to understand the processes during Hg bioaccumulation by terrestrial vegetation.

In this study, atmospheric Hg samples were collected over a period of nearly two years for isotopic composition analysis at two remote mountain sites (Mt. Damei, Zhejiang province in eastern China and Mt. Ailao, Yunnan province in southwest China), three urban/industrial sites in Guiyang (Guizhou province, southwest China) and one urban site in Beijing (north China). Litterfall samples in the forest at the two mountain sites were also collected monthly for stable Hg isotope measurements. The objectives of this study are to (1) characterize the isotopic signatures of atmospheric Hg and litterfall samples at representative remote/urban/industrialized sites in China; (2) investigate Hg isotopic fractionation caused by atmospheric processes (e.g., transportation and transformation); and (3) quantify the magnitude of isotopic fractionation during Hg accumulation in foliage.

EXPERIMENTAL SECTION

Sites Description. As shown in Figure S1 (Supporting Information, SI), Ailaoshan Station for Subtropical Forest Ecosystem Studies (ALS, 24°32'N, 101°01'E, 2491 m a.s.l., operated by Chinese Academy of Sciences) is located at the northern ridge of Mt. Ailao Nature Reserve, Yunnan Province. Around ALS, there are no large anthropogenic Hg emission sources within a radius of ~100 km.

Dameishan Atmospheric Observatory (DAO, operated by Chinese Academy of Sciences) is located at the summit of Mt. Damei (121°33'E, 29°37'N, 550 m a.s.l.) near the coastal range of Ningbo, Zhejiang Province. The location of DAO is proximate to the Yangtze River Delta region, one of the heaviest industrialized areas in China. Anthropogenic Hg emissions, such as from coal combustion, cement production, steel production, waste incineration, domestic heating and solid waste recycling² contribute to the elevated level of total gaseous mercury (TGM, $5.4 \pm 4.1 \text{ ng m}^{-3}$) in the region,³³ compared to Northern Hemisphere background.³⁴

Air sampling was also conducted at two urban sites (SK, MS) in downtown Guiyang and a third site (BY) in a suburban industrialized area (Figure S1). Guiyang is the capital of Guizhou province. Observations of speciated mercury in its urban air showed elevated TGM concentration ($9.72 \pm 10.2 \text{ ng m}^{-3}$), and seasonally high levels of PBM ($<2.5 \mu\text{m}$) ($368 \pm 276 \text{ pg m}^{-3}$).^{35–37} Domestic coal combustion and large industrial point sources have been identified to dominate the local Hg emissions to air.³⁶ An additional TGM sampling was conducted in central Beijing (BJ) to compare the isotope compositions of TGM in the two cities with distinct meteorological conditions (humid subtropical climate in Guiyang vs dry temperate climate in Beijing). Previous monitoring studies^{33,38} showed elevated TGM concentration in Beijing urban air ($10.4 \pm 3.25 \text{ ng m}^{-3}$). More information is available in the Supporting Information.

Sample Collection. The analysis of stable Hg isotopes for TGM and PBM samples was performed following a published method.³⁹ In this method, TGM and PBM are collected on iodinated carbon (IC) traps and quartz fiber filter, respectively. A detailed description of the sampling apparatus and operation is given in the sample collection section of the Supporting Information. The air sampling system at ALS was initially installed below canopy of the forest but moved to a nearby open field after 12 months of operation to examine the influence of canopy on Hg isotopic composition. Sampling locations at the other study sites was fixed over time. An experimental breakthrough measurement was conducted twice in Guiyang to evaluate the sampling efficiency for TGM over time. A separate Hg vapor analyzer (Tekran 2537B, Tekran Instrument, Canada) was installed to continuously monitor the TGM concentration at both inlet and outlet of the IC trap (mean TGM = 11.94 ng m^{-3}). Breakthrough of Hg vapor was not detected for 30 days of continuous sampling. The TGM concentration at the study sites was several times lower than the level during the breakthrough experiment, and the sampling duration was also shorter (1 to 4 weeks compared to 30 days). Therefore, the breakthrough of Hg vapors for the air samples collected at the study site was highly unlikely. Litterfall samples were collected monthly using a nylon net trap in the forest at the two mountain sites. More details are supplied in the sample collection section of the Supporting Information.

Sample Preconcentration Procedures and Total Hg Concentration Analysis. The collected TGM/PBM samples

were processed using a double-stage offline combustion-trapping technique.^{39–41} A catalyst tube (LECO, USA) was utilized to remove iodine and iodine-containing oxidation products from the IC traps that would otherwise cause negative interference in the subsequent isotope measurements. Ten milliliters of KMnO₄ acid trapping solution¹⁴ was utilized to capture the thermally decomposed Hg. A detailed description of the procedure is given in pre-concentration section of the [Supporting Information](#). The Hg mass in each trapping solution was measured by cold vapor atomic fluorescence spectrometry (CVAFS, model 2500, Tekran Instruments, Canada) following the US-EPA Method 1631.⁴² A series of tests with IC traps being spiked with specified amounts of Hg⁰ from an external mercury vapor calibration unit (Tekran model 2505) were conducted. The Hg recovery after catalyst unit was determined to be $94 \pm 6\%$ (1σ ; $n = 6$), whereas the procedural blanks of IC traps were at 50 ± 23 pg (1σ ; $n = 3$), < 1% of the Hg in the sample.

Hg concentration in the litterfall sample was measured by atomic absorption spectroscopy (RA915+ with a pyrolysis unit Pyro-915+, Lumex, Russia).⁴³ The detection limit for Hg concentration was 0.5 ng g⁻¹. All samples were analyzed in triplicate. Accuracy was assessed using the certified reference material GBW10020 (GSB-11, citrus leaves, China), with an average percent recovery of $106 \pm 8\%$ ($n = 10$). Each vegetation sample was subsequently weighed (~0.5 g) and digested by a 5 mL mixture of HNO₃ and H₂SO₄ (4:1, v/v).

Measurement of Hg Concentration and Isotopic Composition. Hg isotopes were measured by MC-ICPMS (Nu Plasma, Nu instruments, UK) following a published methodology.⁴⁴ Before being introduced into the liquid–vapor separator, each trapping solution sample was treated with 0.2 mL of 20% (m/m) NH₂OH–HCl solution (to discharging remaining MnO₄⁻) and diluted to a concentration of ~1 ng Hg mL⁻¹. Hg concentrations of the diluted samples and bracketing standards (SRM 3133, National Institute of Standards and Technology, diluted in 15% (v/v) aqua regia) were matched within 10%. All samples were analyzed twice in 2 blocks (100 cycles per block and 6 s integration time per cycle). The internal precision (1σ) for the Hg isotopic ratio is lower than 0.1%. Hg isotopic compositions are reported in delta notation (δ) in permil (‰).

$$\delta^{xxx}\text{Hg} = \left[\frac{(^{xxx}\text{Hg}/^{198}\text{Hg})_{\text{sample}}}{(^{xxx}\text{Hg}/^{198}\text{Hg})_{\text{SRM3133}}} - 1 \right] \times 1000 \quad (1)$$

where *xxx* refers to the mass of each isotope between 199 and 202 amu. Following Blum and Bergquist⁴⁵ Hg-MIF is reported in capital delta notation (Δ).

$$\Delta^{199}\text{Hg} = \delta^{199}\text{Hg} - 0.252 \times \delta^{202}\text{Hg} \quad (2)$$

$$\Delta^{200}\text{Hg} = \delta^{200}\text{Hg} - 0.502 \times \delta^{202}\text{Hg} \quad (3)$$

$$\Delta^{201}\text{Hg} = \delta^{201}\text{Hg} - 0.752 \times \delta^{202}\text{Hg} \quad (4)$$

UM-Almadén⁴⁵ (diluted to Hg concentration of 1 ng mL⁻¹ in 3% (v/v) nitric acid) was analyzed as a secondary standard, using the same analytical treatment. The determined isotopic composition of UM-Almadén ($\delta^{202}\text{Hg} = -0.57 \pm 0.17\%$; $\Delta^{199}\text{Hg} = -0.03 \pm 0.08\%$; $\Delta^{200}\text{Hg} = 0.00 \pm 0.05\%$; $\Delta^{201}\text{Hg} = -0.03 \pm 0.11\%$, 2σ ; $n = 12$) compared favorably with literature data.⁴⁵ BCR482 (lichen, Institute for Reference Materials and Measurements) was utilized as a solid reference standard for the PBM and litterfall samples to evaluate the isotopic fractionation during pre-concentration. The determined isotopic composition of BCR482 ($\delta^{202}\text{Hg} = -1.67 \pm 0.16\%$; $\Delta^{199}\text{Hg} = -0.57 \pm 0.10\%$; $\Delta^{200}\text{Hg} = 0.06 \pm 0.08\%$; $\Delta^{201}\text{Hg} = -0.58 \pm 0.09\%$, 2σ ; $n = 7$) was comparable with literature data.⁴⁶ The stated uncertainty of isotopic composition for an individual sample listed in [Table S1](#) and [S2](#) corresponded to the larger standard deviation (2σ) or replicate measurements of either the field sample of the UM-Almadén standard.

Meteorological Data. Hourly meteorological data of Ningbo and Beijing were acquired from China Meteorological Administration (<http://data.cma.cn>). Hourly meteorological data or ALS were measured on site by the Chinese Ecological Research Network.

RESULTS AND DISCUSSION

Concentrations and Isotope Compositions of Hg. Hg concentration and isotopic compositions of air and litterfall samples are illustrated in [Figure 1](#) (data shown in [Tables S1](#) and [S2](#)).

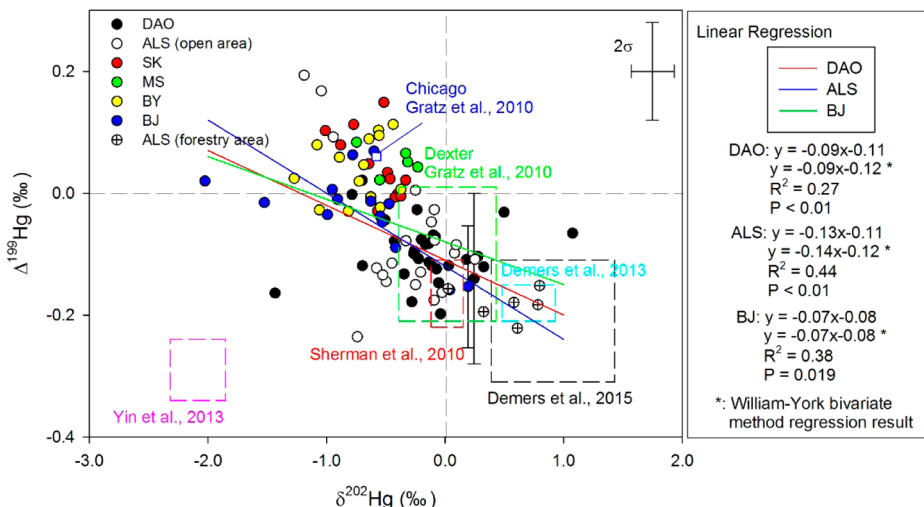


Figure 1. Hg isotopic compositions of TGM, illustrated with reported data ranges from Gratz et al. (2010), Sherman et al. (2010), Demers et al. (2013 and 2015), and Yin et al. (2013), as well as the linear regression lines based on data within 95% confidence intervals from DAO, ALS, and BJ. A bidirectional error bar represent 2σ of replicated isotopic measurements of UM-Almadén and error bars are only marked on dot with 2σ greater than that of UM-Almadén (as elsewhere in the following Figures).

TGM samples collected at ALS were characterized by positive $\delta^{202}\text{Hg}$ and slightly negative $\Delta^{199}\text{Hg}$ ($\delta^{202}\text{Hg}$, $0.52 \pm 0.30\%$; $\Delta^{199}\text{Hg}$, $-0.18 \pm 0.03\%$; 1σ ; $n = 6$), in contrast to the negative $\delta^{202}\text{Hg}$ and near-zero $\Delta^{199}\text{Hg}$ in TGM samples collected at ALS open field ($\delta^{202}\text{Hg}$, $-0.35 \pm 0.39\%$; $\Delta^{199}\text{Hg}$, $-0.07 \pm 0.11\%$; 1σ ; $n = 20$). The isotopic signatures of TGM under canopy agree with the reported data in a forest ecosystem in Wisconsin, USA,²⁶ and a forested peat bog in France.³² Enrico et al.³² observed higher $\delta^{202}\text{Hg}$ and lower TGM at the forested peat bog compared to background Hg and suggested that vegetation removes substantial amounts of TGM by foliage uptake. At ALS, the TGM collected under canopy has higher $\delta^{202}\text{Hg}$ (by 0.9%) compared to the TGM samples collected in the open field, but the concentrations are comparable ($1.6 \pm 0.8 \text{ ng m}^{-3}$; 1σ ; $n = 20$ in open field versus $1.5 \pm 0.2 \text{ ng m}^{-3}$; 1σ ; $n = 6$ under canopy; $p = 0.5$). Demers et al.²⁶ observed highly positive $\delta^{202}\text{Hg}$ in TGM taken from the forest floor. The re-emission from forest floor and foliage uptake by vegetation can both contribute to the positive $\delta^{202}\text{Hg}$ in TGM samples from forest ecosystems.

Negative $\delta^{202}\text{Hg}$ and near-zero $\Delta^{199}\text{Hg}$ were observed in TGM samples ($\delta^{202}\text{Hg}$, $-0.65 \pm 0.37\%$; $\Delta^{199}\text{Hg}$, $0.02 \pm 0.06\%$; 1σ ; $n = 46$) collected at the four urban/industrial sites without significant variation among the three urban sites in Guiyang city, similar to the observations made in the urban air of Chicago, USA.²⁴ Local/regional anthropogenic Hg emissions, especially from coal combustion, are the most important contributor to the TGM in most urban/industrial areas of China.^{2,33,35–37} The isotopic composition of coal being used in the urban area has negative $\delta^{202}\text{Hg}$ and near-zero $\Delta^{199}\text{Hg}$ ($\delta^{202}\text{Hg}$, $-1.00 \pm 0.27\%$ and $\Delta^{199}\text{Hg}$, $-0.03 \pm 0.04\%$ in Guiyang; $\delta^{202}\text{Hg}$, $-1.42 \pm 0.37\%$; $\Delta^{199}\text{Hg}$, $0.05 \pm 0.12\%$ in Beijing).^{47,48} The Hg from coal combustion emission shows up to +0.8% MDF and insignificant MIF.⁴¹ The negative $\delta^{202}\text{Hg}$ and the near-zero $\Delta^{199}\text{Hg}$ in TGM samples observed at the four urban/industrialized sites point to the impact by coal combustion sources.

Negative $\delta^{202}\text{Hg}$ and $\Delta^{199}\text{Hg}$ ($\delta^{202}\text{Hg}$, $-0.16 \pm 0.44\%$; $\Delta^{199}\text{Hg}$, $-0.10 \pm 0.05\%$; 1σ ; $n = 30$) were observed in TGM samples collected at DAO. The broad variation of isotopic composition is evidence of the mixing of background and urban/industrialized air masses (Figure 1).

Negative $\delta^{202}\text{Hg}$ and near-zero $\Delta^{199}\text{Hg}$ ($\delta^{202}\text{Hg}$, $-0.73 \pm 0.54\%$; $\Delta^{199}\text{Hg}$, $0.02 \pm 0.07\%$; 1σ ; $n = 46$) were observed in PBM collected at DAO and the three urban/industrial sites in Guiyang (Figure 2). Similar isotopic compositions in PBM at a landfill site in Kolkata, India, has also been reported by Das et al.⁴⁹ PBM may be from primary sources, such as coal combustion, as well as from secondary processes where gaseous Hg species is absorbed to atmospheric particulates.^{6,50} Since particles are removed faster from air (in hours to a few days) than Hg^0 ,⁶ local and regional emission sources, especially coal combustion in China,⁵¹ are the major contributor to PBM. Coal combustion is most likely the driver for the observed $\delta^{202}\text{Hg}$ and $\Delta^{199}\text{Hg}$ of PBM at these sites. The $\delta^{202}\text{Hg}$ in PBM measured indoor at MS displays considerable differences compared to outdoor air (SK, see PBM between indoor and outdoor air section in the Supporting Information), which warrants further investigation.

In contrast to other studies (see Table S3 for references), discernible (one-way ANOVA, $p < 0.05$) negative even-mass-number isotope MIF ($\Delta^{200}\text{Hg}$, $-0.07 \pm 0.02\%$; 1σ ; $n = 6$) in TGM was found only under canopy at ALS. These samples were collected near the forest floor, where Demers et al.²⁶ in a study at the Rhineland FACE site found negative $\Delta^{200}\text{Hg}$ ($-0.10 \pm 0.02\%$) in TGM, in contrast to the TGM samples collected above

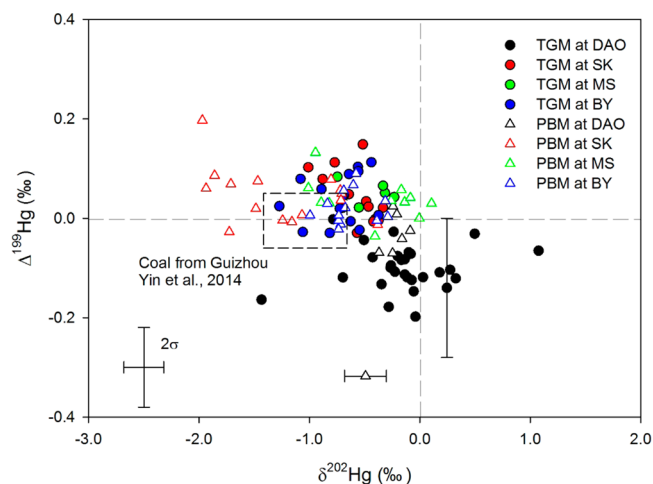


Figure 2. Comparison of Hg isotopic compositions in PBM and TGM samples from DAO and three urban sites in Guiyang city (SK, MS, BY), illustrated with reported data ranges from Yin et al. (2014).

the canopy in the same study. It has been hypothesized that significant $\Delta^{200}\text{Hg}$ in TGM is indicative of long-range transport from the upper troposphere.²⁷ Nevertheless, the processes triggering the $\Delta^{200}\text{Hg}$ have not been elucidated.

A significant (t -test, $P < 0.01$) negative shift was observed for both $\delta^{202}\text{Hg}$ and $\Delta^{199}\text{Hg}$ in litterfall samples in comparison to the TGM samples at the two mountain sites (litterfall samples at ALS, $\delta^{202}\text{Hg}$, $-3.03 \pm 0.28\%$; $\Delta^{199}\text{Hg}$, $-0.40 \pm 0.08\%$; 1σ ; $n = 73$; at DAO, $\delta^{202}\text{Hg}$, $-2.52 \pm 0.67\%$; $\Delta^{199}\text{Hg}$, $-0.22 \pm 0.10\%$; 1σ ; $n = 11$). This implies that both (–)MDF and (–)MIF occur during foliage assimilation of atmospheric Hg or postdeposition transformations. Recent studies^{23,26,32,52} have reported relatively lower $\delta^{202}\text{Hg}$ and $\Delta^{199}\text{Hg}$ in vegetation samples (e.g., aspen, rice, moss, pine, shrub, and lichen species) compared to the values in ambient air samples. Hg isotopic compositions in litter at ALS are more negative $\Delta^{199}\text{Hg}$ compared to the samples at the DAO site, without significant variation among the major defoliating tree species, which implies that similar isotopic compositions may be observed in foliage from different tree species.

Binary Mixing Trend of Isotopic Compositions in TGM and Litterfall Samples. The difference (t test, $p < 0.01$) of the $\delta^{202}\text{Hg}$ and $\Delta^{199}\text{Hg}$ values among the air samples collected at ALS forest and Guiyang exhibits the influence by anthropogenic and natural emission sources of Hg. The attribution of source origin using measurements of Hg isotopic composition in precipitation, lichen, and soil samples has been demonstrated previously.^{24,53,54}

Atmospheric Hg from immediate anthropogenic emissions is characterized by negative $\delta^{202}\text{Hg}$ and near-zero $\Delta^{199}\text{Hg}$, while Hg associated with regional background displays more positive $\delta^{202}\text{Hg}$ and negative $\Delta^{199}\text{Hg}$ (Table S3). The linear regression analysis of $\Delta^{199}\text{Hg}/\delta^{202}\text{Hg}$ ratio in TGM samples collected at DAO, ALS, and BJ sites is given in Figure 1. A William–York bivariate method⁵⁵ was also applied for linear regression corresponding isotopic data with 2σ to show the potential influences of data variability in the regression. The slope and intercept of the regression lines are also consistent with the TGM isotopic data reported earlier.^{23,24,26,27,56} We hypothesized that the trend represents the mixing of the global background TGM pool and anthropogenic TGM emissions. Redox cycling, diffusion, and mixing processes, as well as the surface exchange between air and land/ocean surface result in a homogeneous Hg isotopic composition pool. In contrast, anthropogenic emissions, mostly

inherited from fossil fuel combustion, may shift the isotopic composition in ambient air.

For the air samples under influence of anthropogenic emission sources, the $\Delta^{199}\text{Hg}$ and ambient TGM concentrations are correlated linearly (Figure 4). At higher TGM concentration, $\Delta^{199}\text{Hg}$

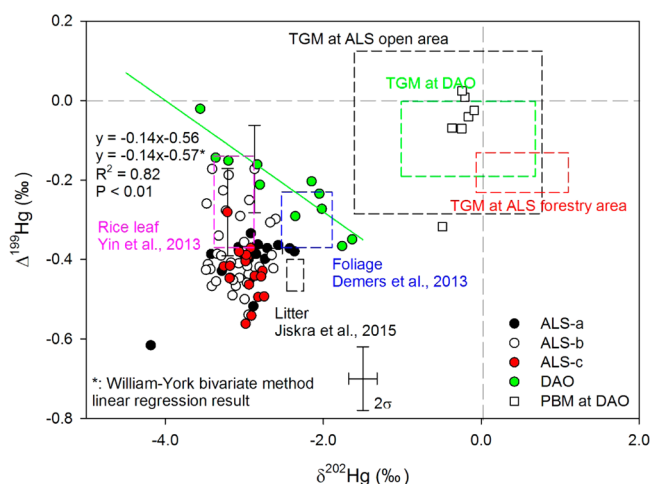


Figure 3. Hg isotopic compositions in litterfall samples collected at two remote mountain sites (DAO and ALS), compared with reported data ranges from Yin et al. (2013), Demers et al. (2013), and Jiskra et al. (2015), and the Hg isotopic compositions in air samples at the sites, with a linear regression line for data in litter samples at DAO (ALS-a, mixing species samples; ALS-b, *Manglietia insignis*; ALS-c, *Lithocarpus chintungensis*).

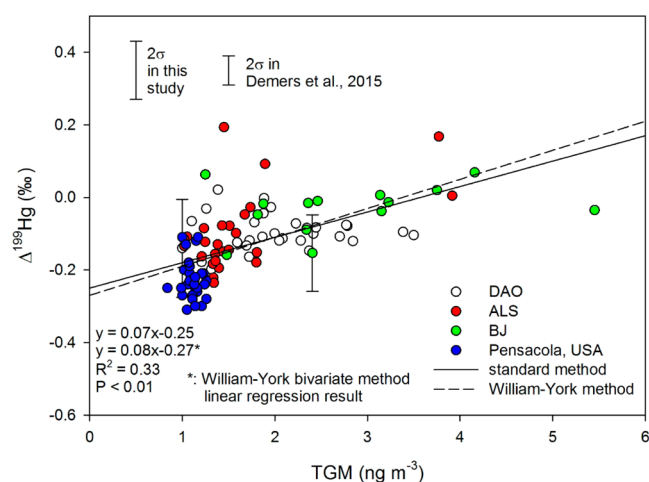


Figure 4. Relationship between $\Delta^{199}\text{Hg}$ and Hg concentration in TGM samples from DAO, ALS, and BJ, plotted with data reported by Demers et al. (2015) and linear regression results.

increases and gradually approaches zero as anthropogenic Hg emissions. In turn, negative $\Delta^{199}\text{Hg}$ corresponds to lower TGM concentrations commonly observed at remote areas. The linear regression result gives ca. -0.15% at a Hg concentration of 1.5 ng m^{-3} , which represents the background atmospheric Hg concentration in the northern hemisphere.

It should be noted that there are data points deviating from the regression lines in Figures 1 and 4. The most likely reason is the impact of additional atmospheric Hg sources with distinct isotopic composition. Influences by photochemistry may also shift the isotopic composition (see the section in the Supporting Information, Sunlight exposure influence the $\Delta^{199}\text{Hg}$ in TGM).

For the TGM at BJ, the influences from atmospheric processes are diluted due to the elevated TGM concentration from nearby anthropogenic emissions. The data scattering in Figures 1 and 4 are mostly those observed at DAO and ALS, where photochemical reactions and other atmospheric Hg processes could shift the isotopic compositions. More fundamental research and field observations are necessary to understand the causes of these deviations in Hg isotopic composition.

Hg isotopic composition in foliage are inherited from ambient air with modification during uptake processes.^{26,32} Nevertheless, foliage is not a passive isotopic monitor of TGM because the uptake induces a considerable shift in Hg isotopic composition. The fractionation process is indicated by the linear fit aligning the deciduous foliage data from DAO in the Δ - δ space that shows a similar slope between the Hg isotopic composition in litterfall collected at DAO and the isotopic compositions in TGM (Figure 3). The isotopic signatures ($\Delta^{199}\text{Hg}$ and $\delta^{202}\text{Hg}$) and the Hg concentration in litterfall collected at DAO is shown in Figure 5. The higher Hg concentration in litter is most possibly

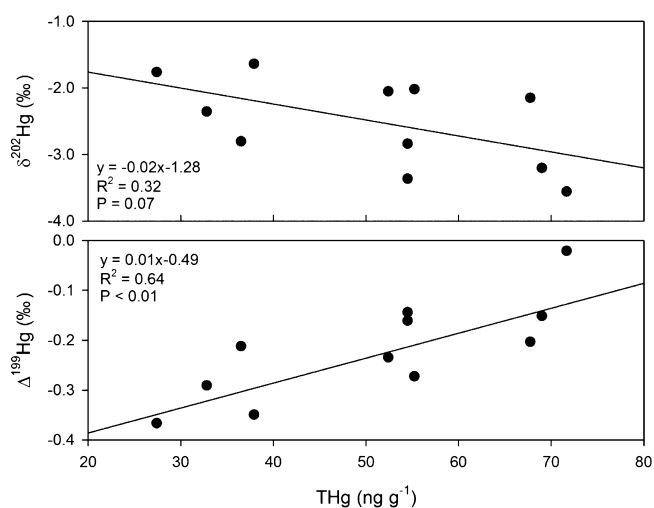


Figure 5. Relationship between Hg isotopic composition signatures ($\delta^{202}\text{Hg}$ and $\Delta^{199}\text{Hg}$) and Hg concentration in litter collected at DAO.

caused by the uptake of Hg of anthropogenic sources, leading to the associations of high Hg concentration with the $\delta^{202}\text{Hg}$ and $\Delta^{199}\text{Hg}$ signatures from anthropogenic Hg emissions. The samples collected at ALS are subject to a weaker influence of anthropogenic emissions compared to the samples collected at DAO. The vegetation at ALS is of evergreen broad-leaf species with 0.9–2.4 yr foliage lifespan, compared to ~ 1 yr of lifespan for deciduous species at DAO. This dilutes the influence of the anthropogenic emissions on the Hg isotopic signature found in the litter at ALS. The dark abiotic reduction or photochemical reactions of Hg in foliage/litter may also pose an effect to the isotopic compositions in litterfall samples.

Mechanism Responsible for the Observed Hg-MIF. MIF of Hg isotopes are primarily explained by two mechanisms: the nuclear volume effect (NVE) and magnetic isotope effects (MIE).^{7,57,58} Previous studies^{10,12,15,59} indicate that MIF caused by NVE produces a slope of ~ 1.6 in the scatter plot of $\Delta^{199}\text{Hg}$ versus $\Delta^{201}\text{Hg}$, while MIE by photochemical reduction of $\text{Hg}^{2+}(\text{aq})$ yields a slope near unity (~ 1.0).⁷ The MIF in TGM samples is a result of multiple processes including emissions, atmospheric mixing, and photochemical processes during transport/transformation; and the MIF signatures in litter are

from atmospheric Hg with modification by uptake. Figure S2 shows the ratios of $\Delta^{201}\text{Hg}/\Delta^{199}\text{Hg}$ for all TGM and litterfall samples. The $\Delta^{199}\text{Hg}$ vs $\Delta^{201}\text{Hg}$ plot aligns linearly ($p < 0.01$) with a slope of near unity, implying that MIE is primarily responsible for the observed MIF. This suggests that TGM and the Hg accumulated by foliage is subject to photochemical reactions.^{24,26,60–62} However, at locations proximate to anthropogenic emission sources, the negative MIF may be influenced by mixing with polluted air with near-zero MIF signatures. At remote locations, the negative Hg-MIF signatures are clearly manifest. The MIF signatures in TGM are a result of multiple processes, that is, volatilization, air mixing and photochemical reactions; while the MIF signatures in litter are inherited from atmospheric Hg, with modification by the uptake.

Negative $\delta^{202}\text{Hg}$ and positive $\Delta^{199}\text{Hg}$ observed in rainfall samples have been reported.^{25,63,64} Given the Hg isotopic fractionation observed in rainwater and PBM (negative $\delta^{202}\text{Hg}$ and near-zero $\Delta^{199}\text{Hg}$ in this study), it is unlikely that the Hg in litterfall samples is derived from PBM or wet deposition. The most likely reason for the negative MIF shift from ambient air to litter is the re-emission of Hg from foliage/litterfall, possibly caused by redox processes.⁶⁵ Although the transformation of Hg within foliage remains unclear, photoreduction of Hg^{2+} bound to reduced sulfur groups may yield (–)MIF.¹⁰ Alternative possibilities including the oxidation of Hg^0 in stoma, atmospheric Hg transformation, and mixing with Hg^{2+} transported from root area inside the vesicular plant, may also contribute to the MIF shift between atmospheric Hg and Hg in litter.

Implications. This is the first study reporting the isotopic compositions in TGM and PBM, as well as litter-bound Hg in mainland China. We illustrated that atmospheric Hg from anthropogenic emissions and natural background differ in stable Hg isotopes. The influences of multiple sources/processes on the isotopic compositions of TGM are diluted at sites subject to anthropogenic emissions. Both MDF and MIF occur during Hg uptake in foliage, resulting in more negative $\delta^{202}\text{Hg}$ and $\Delta^{199}\text{Hg}$ in litter. The primary mechanism responsible for the observed MIF in TGM and litter-bound Hg is MIE induced by photochemical reactions. The isotopic signatures of Hg (including MDF and MIF) help identify the Hg sources and biogeochemical processes. However, the limited temporal resolution of the atmospheric Hg samples impairs the ability to determine the actual processes involved in shifting the isotopic fractionation signatures. Collection with a higher temporal resolution (e.g., on a weekly or daily basis) can enable exploration of isotopic composition of stable Hg caused by emission and/or transformation events. Procedures may include chlorinated carbon (CIC) traps modified for high rate sampling³⁹ or synchronous sampling on multiple traps in parallel to collect sufficient TGM required for isotopic measurements.

■ ASSOCIATED CONTENT

📄 Supporting Information

The Supporting Information is available free of charge on the ACS Publications website at DOI: 10.1021/acs.est.6b01782.

Site description; sample collection; preconcentration; PBM between indoor and outdoor air; sunlight exposure influence; supplementary figures and tables (PDF)

■ AUTHOR INFORMATION

Corresponding Authors

*Phone: +86 851 85891508; fax: +86 851 85891609; email: fuxuewu@mail.gyig.ac.cn (Xuewu Fu).

*Phone: +86 851 85891356; fax: +86 851 85891609; email: shanglihai@vip.skleg.cn (Lihai Shang).

*Phone: +86 851 85895728; fax: +86 851 85891609; email: fengxinbin@vip.skleg.cn (Xinbin Feng).

Notes

The authors declare no competing financial interest.

■ ACKNOWLEDGMENTS

This work was supported by National “973” Program (2013CB430003), Natural Science Foundation of China (41173024 and 41473025), the innovation and collaboration program of Chinese Academy of Sciences, and Strategic Priority Research Program B of the Chinese Academy of Sciences (Grant No. XDB05030304), inspired from the Research Program RIMNES funded by the French Research Agency (ANR-11-CESA-0013) and the European Research Council (ERC-2010-StG_20091028). We also thank Dameishan Atmosphere Observatory, Ailaoshan Station, for Subtropical Forest Ecosystem Studies, Institute of Atmospheric Physics and Guangzhou Institute of Geochemistry, Chinese Academy of Sciences, for field sampling assistance, as well as State Key Laboratory of Marine Environmental Science, Xiamen University, for isotopic analyzing assistance.

■ REFERENCES

- (1) UNEP *Global Mercury Assessment 2013: Sources, Emissions, Releases and Environmental Transport*; UNEP Chemicals Branch Geneva: Switzerland, 2013.
- (2) Streets, D. G.; Hao, J. M.; Wu, Y.; Jiang, J. K.; Chan, M.; Tian, H. Z.; Feng, X. B. Anthropogenic mercury emissions in China. *Atmos. Environ.* **2005**, *39* (40), 7789–7806.
- (3) Fu, X. W.; Zhang, H.; Yu, B.; Wang, X.; Lin, C. J.; Feng, X. B. Observations of atmospheric mercury in China: a critical review. *Atmos. Chem. Phys.* **2015**, *15* (16), 9455–9476.
- (4) Gustin, M. S.; Jaffe, D. A. Reducing the uncertainty in measurement and understanding of mercury in the atmosphere. *Environ. Sci. Technol.* **2010**, *44* (7), 2222–2227.
- (5) Zhu, W.; Sommar, J.; Lin, C. J.; Feng, X. Mercury vapor air–surface exchange measured by collocated micrometeorological and enclosure methods - Part I: Data comparability and method characteristics. *Atmos. Chem. Phys.* **2015**, *15* (2), 685–702.
- (6) Schroeder, W. H.; Munthe, J. Atmospheric mercury—an overview. *Atmos. Environ.* **1998**, *32* (5), 809–822.
- (7) Bergquist, B. A.; Blum, J. D. Mass-dependent and -independent fractionation of Hg isotopes by photoreduction in aquatic systems. *Science* **2007**, *318* (5849), 417–420.
- (8) Zheng, W.; Hintelmann, H. Mercury isotope fractionation during photoreduction in natural water is controlled by its Hg/DOC ratio. *Geochim. Cosmochim. Acta* **2009**, *73* (22), 6704–6715.
- (9) Yang, L.; Sturgeon, R. E. Isotopic fractionation of mercury induced by reduction and ethylation. *Anal. Bioanal. Chem.* **2009**, *393* (1), 377–385.
- (10) Zheng, W.; Hintelmann, H. Isotope fractionation of mercury during its photochemical reduction by low-molecular-weight organic compounds. *J. Phys. Chem. A* **2010**, *114* (12), 4246–4253.
- (11) Malinovsky, D.; Latruwe, K.; Moens, L.; Vanhaecke, F. Experimental study of mass-independence of Hg isotope fractionation during photodecomposition of dissolved methylmercury. *J. Anal. At. Spectrom.* **2010**, *25* (7), 950–956.
- (12) Estrade, N.; Carignan, J.; Sonke, J. E.; Donard, O. F. Mercury isotope fractionation during liquid–vapor evaporation experiments. *Geochim. Cosmochim. Acta* **2009**, *73* (10), 2693–2711.

- (13) Ghosh, S.; Schauble, E. A.; Lacrampe Couloume, G.; Blum, J. D.; Bergquist, B. A. Estimation of nuclear volume dependent fractionation of mercury isotopes in equilibrium liquid–vapor evaporation experiments. *Chem. Geol.* **2013**, *336*, 5–12.
- (14) Zheng, W.; Foucher, D.; Hintelmann, H. Mercury isotope fractionation during volatilization of Hg(0) from solution into the gas phase. *J. Anal. At. Spectrom.* **2007**, *22* (9), 1097–1104.
- (15) Wiederhold, J. G.; Cramer, C. J.; Daniel, K.; Infante, I.; Bourdon, B.; Kretzschmar, R. Equilibrium Mercury Isotope Fractionation between Dissolved Hg(II) Species and Thiol-Bound Hg. *Environ. Sci. Technol.* **2010**, *44* (11), 4191–4197.
- (16) Jiskra, M.; Wiederhold, J. G.; Bourdon, B.; Kretzschmar, R. Solution Speciation Controls Mercury Isotope Fractionation of Hg(II) Sorption to Goethite. *Environ. Sci. Technol.* **2012**, *46* (12), 6654–6662.
- (17) Koster van Groos, P. G.; Esser, B. K.; Williams, R. W.; Hunt, J. R. Isotope effect of mercury diffusion in air. *Environ. Sci. Technol.* **2014**, *48* (1), 227–233.
- (18) Rodriguez-Gonzalez, P.; Epov, V. N.; Bridou, R.; Tessier, E.; Guyoneaud, R.; Monperrus, M.; Amouroux, D. Species-specific stable isotope fractionation of mercury during Hg(II) methylation by an anaerobic bacteria (*Desulfobulbus propionicus*) under dark conditions. *Environ. Sci. Technol.* **2009**, *43* (24), 9183–9188.
- (19) Jiménez-Moreno, M.; Perrot, V.; Epov, V. N.; Monperrus, M.; Amouroux, D. Chemical kinetic isotope fractionation of mercury during abiotic methylation of Hg(II) by methylcobalamin in aqueous chloride media. *Chem. Geol.* **2013**, *336* (0), 26–36.
- (20) Kritee, K.; Barkay, T.; Blum, J. D. Mass dependent stable isotope fractionation of mercury during mer mediated microbial degradation of monomethylmercury. *Geochim. Cosmochim. Acta* **2009**, *73* (5), 1285–1296.
- (21) Kritee, K.; Blum, J. D.; Johnson, M. W.; Bergquist, B. A.; Barkay, T. Mercury stable isotope fractionation during reduction of Hg(II) to Hg(0) by mercury resistant microorganisms. *Environ. Sci. Technol.* **2007**, *41* (6), 1889–1895.
- (22) Kritee, K.; Blum, J. D.; Barkay, T. Mercury stable isotope fractionation during reduction of Hg(II) by different microbial pathways. *Environ. Sci. Technol.* **2008**, *42* (24), 9171–9177.
- (23) Yin, R.; Feng, X.; Meng, B. Stable mercury isotope variation in rice plants (*Oryza sativa* L.) from the Wanshan mercury mining district, SW China. *Environ. Sci. Technol.* **2013**, *47* (5), 2238–2245.
- (24) Gratz, L. E.; Keeler, G. J.; Blum, J. D.; Sherman, L. S. Isotopic composition and fractionation of mercury in Great Lakes precipitation and ambient air. *Environ. Sci. Technol.* **2010**, *44* (20), 7764–7770.
- (25) Chen, J. B.; Hintelmann, H.; Feng, X. B.; Dimock, B. Unusual fractionation of both odd and even mercury isotopes in precipitation from Peterborough, ON, Canada. *Geochim. Cosmochim. Acta* **2012**, *90*, 33–46.
- (26) Demers, J. D.; Blum, J. D.; Zak, D. R. Mercury isotopes in a forested ecosystem: Implications for air-surface exchange dynamics and the global mercury cycle. *Global Biogeochemical Cycles* **2013**, *27* (1), 222–238.
- (27) Demers, J. D.; Sherman, L. S.; Blum, J. D.; Marsik, F. J.; Dvonch, J. T. Coupling atmospheric mercury isotope ratios and meteorology to identify sources of mercury impacting a coastal urban-industrial region near Pensacola, Florida, USA. *Global Biogeochemical Cycles* **2015**, *29* (10), 1689–1705.
- (28) Sun, R.; Streets, D. G.; Horowitz, H. M.; Amos, H. M.; Liu, G.; Perrot, V.; Toutain, J.-P.; Hintelmann, H.; Sunderland, E. M.; Sonke, J. E. Historical (1850–2010) mercury stable isotope inventory from anthropogenic sources to the atmosphere. *Elementa: Science of the Anthropocene* **2016**, *4* (1), 000091.
- (29) Rolison, J. M.; Landing, W. M.; Luke, W.; Cohen, M.; Salters, V. J. M. Salters, V. J. M., Isotopic composition of species-specific atmospheric Hg in a coastal environment. *Chem. Geol.* **2013**, *336*, 37–49.
- (30) Tsui, M. T.; Blum, J. D.; Kwon, S. Y.; Finlay, J. C.; Balogh, S. J.; Nollet, Y. H. Sources and transfers of methylmercury in adjacent river and forest food webs. *Environ. Sci. Technol.* **2012**, *46* (20), 10957–10964.
- (31) Carignan, J.; Estrade, N.; Sonke, J. E.; Donard, O. F. Odd isotope deficits in atmospheric Hg measured in lichens. *Environ. Sci. Technol.* **2009**, *43* (15), 5660–5664.
- (32) Enrico, M.; Roux, G. L.; Maruszczak, N.; Heimbürger, L.-E.; Claustres, A.; Fu, X.; Sun, R.; Sonke, J. E. Atmospheric Mercury Transfer to Peat Bogs Dominated by Gaseous Elemental Mercury Dry Deposition. *Environ. Sci. Technol.* **2016**, *50* (5), 2405–2412.
- (33) Wang, Z. W.; Chen, Z. S.; Duan, N.; Zhang, X. S. Gaseous elemental mercury concentration in atmosphere at urban and remote sites in China. *J. Environ. Sci.* **2007**, *19* (2), 176–180.
- (34) Sprovieri, F.; Pirrone, N.; Ebinghaus, R.; Kock, H.; Dommergue, A. A review of worldwide atmospheric mercury measurements. *Atmos. Chem. Phys.* **2010**, *10* (17), 8245–8265.
- (35) Feng, X. B.; Shang, L. H.; Wang, S. F.; Tang, S. L.; Zheng, W. Temporal variation of total gaseous mercury in the air of Guiyang, China. *J. Geophys. Res.-Atmos.* **2004**, *109*, 04159 DOI: 10.1029/2003JD004159.
- (36) Fu, X. W.; Feng, X. B.; Qiu, G. L.; Shang, L. H.; Zhang, H. Speciated atmospheric mercury and its potential source in Guiyang, China. *Atmos. Environ.* **2011**, *45* (25), 4205–4212.
- (37) Liu, N.; Qiu, G. G.; Landis, M. S.; Feng, X. B.; Fu, X. W.; Shang, L. H. Atmospheric mercury species measured in Guiyang, Guizhou province, southwest China. *Atmos. Res.* **2011**, *100* (1), 93–102.
- (38) Liu, S.; Nadim, F.; Perkins, C.; Carley, R. J.; Hoag, G. E.; Lin, Y.; Chen, L. Atmospheric mercury monitoring survey in Beijing, China. *Chemosphere* **2002**, *48* (1), 97–107.
- (39) Fu, X. W.; Heimbürger, L. E.; Sonke, J. E. Collection of atmospheric gaseous mercury for stable isotope analysis using iodine- and chlorine-impregnated activated carbon traps. *J. Anal. At. Spectrom.* **2014**, *29* (5), 841–852.
- (40) Sun, R.; Enrico, M.; Heimbürger, L.-E.; Scott, C.; Sonke, J. E. A double-stage tube furnace—acid-trapping protocol for the pre-concentration of mercury from solid samples for isotopic analysis. *Anal. Bioanal. Chem.* **2013**, *405* (21), 6771–6781.
- (41) Sun, R.; Heimbürger, L.-E.; Sonke, J. E.; Liu, G.; Amouroux, D.; Beraïl, S. Mercury stable isotope fractionation in six utility boilers of two large coal-fired power plants. *Chem. Geol.* **2013**, *336*, 103–111.
- (42) *Method 1631, Revision E: Mercury in water by oxidation, purge and trap, and cold vapor atomic fluorescence spectrometry*; US Environmental Protection Agency: Washington, DC, 2002.
- (43) Rodriguez, L.; Rincon, J.; Asencio, I.; Rodriguez-Castellanos, L. Capability of selected crop plants for shoot mercury accumulation from polluted soils: phytoremediation perspectives. *Int. J. Phytorem.* **2007**, *9* (1), 1–13.
- (44) Yin, R.; Feng, X.; Foucher, D.; Shi, W.; Zhao, Z.; Wang, J. High precision determination of mercury isotope ratios using online mercury vapor generation system coupled with multicollector inductively coupled plasma-mass spectrometer. *Chinese Journal of Analytical Chemistry* **2010**, *38* (7), 929–934.
- (45) Blum, J. D.; Bergquist, B. A. Reporting of variations in the natural isotopic composition of mercury. *Anal. Bioanal. Chem.* **2007**, *388* (2), 353–359.
- (46) Estrade, N.; Carignan, J.; Sonke, J. E.; Donard, O. F. Measuring Hg Isotopes in Bio-Geo-Environmental Reference Materials. *Geostand. Geoanal. Res.* **2010**, *34* (1), 79–93.
- (47) Biswas, A.; Blum, J. D.; Bergquist, B. A.; Keeler, G. J.; Xie, Z. Natural mercury isotope variation in coal deposits and organic soils. *Environ. Sci. Technol.* **2008**, *42* (22), 8303–8309.
- (48) Yin, R.; Feng, X.; Chen, J. Mercury Stable Isotopic Compositions in Coals from Major Coal Producing Fields in China and Their Geochemical and Environmental Implications. *Environ. Sci. Technol.* **2014**, *48* (10), 5565–5574.
- (49) Das, R.; Wang, X.; Khezri, B.; Webster, R. D.; Sikdar, P. K.; Datta, S. Mercury isotopes of atmospheric particle bound mercury for source apportionment study in urban Kolkata, India. *Elementa: Science of the Anthropocene* **2016**, *4*, 000098.
- (50) Keeler, G.; Glinsorn, G.; Pirrone, N. Particulate Mercury in the Atmosphere - Its Significance, Transport, Transformation and Sources. *Water, Air, Soil Pollut.* **1995**, *80* (1–4), 159–168.

(51) Pirrone, N.; Cinnirella, S.; Feng, X.; Finkelman, R. B.; Friedli, H. R.; Leaner, J.; Mason, R.; Mukherjee, A. B.; Stracher, G. B.; Streets, D. G.; Telmer, K. Global mercury emissions to the atmosphere from anthropogenic and natural sources. *Atmos. Chem. Phys.* **2010**, *10* (13), 5951–5964.

(52) Jiskra, M.; Wiederhold, J. G.; Skyllberg, U.; Kronberg, R.-M.; Hajdas, I.; Kretzschmar, R. Mercury Deposition and Re-emission Pathways in Boreal Forest Soils Investigated with Hg Isotope Signatures. *Environ. Sci. Technol.* **2015**, *49* (12), 7188–7196.

(53) Estrade, N.; Carignan, J.; Donard, O. F. Isotope tracing of atmospheric mercury sources in an urban area of northeastern France. *Environ. Sci. Technol.* **2010**, *44* (16), 6062–6067.

(54) Estrade, N.; Carignan, J.; Donard, O. F. Tracing and quantifying anthropogenic mercury sources in soils of northern France using isotopic signatures. *Environ. Sci. Technol.* **2011**, *45* (4), 1235–1242.

(55) Cantrell, C. A. Technical Note: Review of methods for linear least-squares fitting of data and application to atmospheric chemistry problems. *Atmos. Chem. Phys.* **2008**, *8* (17), 5477–5487.

(56) Sherman, L. S.; Blum, J. D.; Johnson, K. P.; Keeler, G. J.; Barres, J. A.; Douglas, T. A. Mass-independent fractionation of mercury isotopes in Arctic snow driven by sunlight. *Nat. Geosci.* **2010**, *3* (3), 173–177.

(57) Schauble, E. A. Role of nuclear volume in driving equilibrium stable isotope fractionation of mercury, thallium, and other very heavy elements. *Geochim. Cosmochim. Acta* **2007**, *71* (9), 2170–2189.

(58) Sonke, J. E. A global model of mass independent mercury stable isotope fractionation. *Geochim. Cosmochim. Acta* **2011**, *75* (16), 4577–4590.

(59) Zheng, W.; Hintelmann, H. Nuclear field shift effect in isotope fractionation of mercury during abiotic reduction in the absence of light. *J. Phys. Chem. A* **2010**, *114* (12), 4238–4245.

(60) Zhang, H.; Lindberg, S. E. Processes influencing the emission of mercury from soils: A conceptual model. *J. Geophys Res-Atmos* **1999**, *104* (D17), 21889–21896.

(61) Yin, R.; Feng, X.; Li, X.; Yu, B.; Du, B. Trends and advances in mercury stable isotopes as a geochemical tracer. *Trends Environ. Anal. Chem.* **2014**, *2* (0), 1–10.

(62) Blum, J. D.; Sherman, L. S.; Johnson, M. W. Mercury Isotopes in Earth and Environmental Sciences. *Annu. Rev. Earth Planet. Sci.* **2014**, *42* (0), 249–269.

(63) Wang, Z.; Chen, J.; Feng, X.; Hintelmann, H.; Yuan, S.; Cai, H.; Huang, Q.; Wang, S.; Wang, F. Mass-dependent and mass-independent fractionation of mercury isotopes in precipitation from Guiyang, SW China. *C. R. Geosci.* **2015**, *347* (7–8), 358–367.

(64) Yuan, S.; Zhang, Y.; Chen, J.; Kang, S.; Zhang, J.; Feng, X.; Cai, H.; Wang, Z.; Wang, Z.; Huang, Q. Large Variation of Mercury Isotope Composition During a Single Precipitation Event at Lhasa City, Tibetan Plateau, China. *Procedia Earth Planet. Sci.* **2015**, *13*, 282–286.

(65) Rutter, A. P.; Schauer, J. J.; Shafer, M. M.; Creswell, J. E.; Olson, M. R.; Robinson, M.; Collins, R. M.; Parman, A. M.; Katzman, T. L.; Mallek, J. L. Dry deposition of gaseous elemental mercury to plants and soils using mercury stable isotopes in a controlled environment. *Atmos. Environ.* **2011**, *45* (4), 848–855.